

The immunoglobulin-like protein Hibris functions as a dose-dependent regulator of myoblast fusion and is differentially controlled by Ras and Notch signaling

Ruben D. Artero, Irinka Castanon and Mary K. Baylies*

Molecular Biology Program, Sloan-Kettering Institute, Memorial Sloan-Kettering Cancer Center, 1275 York Avenue, New York, NY 10021, USA

*Author for correspondence (e-mail: m-baylies@ski.mskcc.org)

Accepted 14 August 2001

SUMMARY

Hibris (Hbs) is a transmembrane immunoglobulin-like protein that shows extensive homology to *Drosophila* Sticks and stones (Sns) and human kidney protein Nephric. Hbs is expressed in embryonic visceral, somatic and pharyngeal mesoderm among other tissues. In the somatic mesoderm, Hbs is restricted to fusion competent myoblasts and is regulated by Notch and Ras signaling pathways. Embryos that lack or overexpress *hbs* show a partial block of myoblast fusion, followed by abnormal muscle morphogenesis. Abnormalities in visceral mesoderm are also observed. In vivo mapping of functional domains suggests that the intracellular domain mediates Hbs activity. Hbs and its paralog, Sns, co-localize at the cell membrane of fusion-competent myoblasts. The two

proteins act antagonistically: loss of *sns* dominantly suppresses the *hbs* myoblast fusion and visceral mesoderm phenotypes, and enhances Hbs overexpression phenotypes. Data from a P-homed enhancer reporter into *hbs* and co-localization studies with Sns suggest that *hbs* is not continuously expressed in all fusion-competent myoblasts during the fusion process. We propose that the temporal pattern of *hbs* expression within fusion-competent myoblasts may reflect previously undescribed functional differences within this myoblast population.

Key words: Myoblast fusion, Mesoderm, Morphogenesis, Sticks and stones, Hbs, *Drosophila*

INTRODUCTION

In *Drosophila*, each larval body wall muscle acquires a distinct set of morphological traits during embryogenesis that provides the unique identity of the muscle within the organism. These traits include the size, which is governed by the number of fusion events, the shape, which is controlled by attachment site choice and cytoskeletal dynamics, and the innervation pattern, which is guided by interactions between recognition proteins on the muscle and motoneuron surface.

Part of the diversity in muscle identity stems from specification of two sets of myoblasts. Founder myoblasts contain the information required for morphogenesis of a given muscle, while fusion-competent myoblasts are believed to be naïve myoblasts that fuse progressively to a founder cell and become entrained to a particular muscle program (Bate, 1990; Dohrmann et al., 1990). This notion is supported by analysis of fusion mutants such as *myoblast city* (Rushton et al., 1995; Erickson et al., 1997) in which founder cells execute aspects of their individual morphogenetic programs (e.g. attract the appropriate motoneuron), whereas fusion competent cells apoptose, suggesting that no specific developmental instructions have been received. A combination of signals from

the ectoderm and mesoderm ultimately lead to segregation of both myoblast types (Frasch, 1999; Baylies and Michelson, 2001). The intersection of Wingless and Decapentaplegic activities defines a region in the dorsal mesoderm that is competent to respond to inductive signals mediated by the Ras signaling pathway. The localized activation of Ras in this region instructs clusters of myoblasts to adopt the founder cell fate (Carmena et al., 1998a; Buff et al., 1998; Wilson, 1999). This fate is restricted to a single cell within each cluster, the muscle progenitor, by a process of lateral inhibition mediated by the Notch and Delta signaling pathway (Corbin et al., 1991; Bate et al., 1993; Carmena et al., 1995). Cells that receive the Delta signal from a neighboring muscle progenitor segregate as fusion-competent cells. Muscle progenitors then divide asymmetrically to form founder cells (Ruiz-Gomez and Bate, 1997; Carmena et al., 1998b). The specific combination of signals that a given founder cell receives results in activation of a particular set of transcription factors such as Krüppel or Even-skipped (Ruiz-Gómez et al., 1997; Carmena et al., 1998a; Halfon et al., 2000), which, in turn, regulate the attributes characteristic for each muscle. Fusion-competent cells, which result from the activation of Notch, start expressing proteins such as Sticks and Stones (Sns) (Bour et al., 2000) that are

required for their subsequent differentiation. However, we know little about how these transcription factors determine identity and how fusion-competent cells contribute to this process. Even though it is generally assumed that fusion-competent cells are naïve and contribute only mass to the muscle, it is formally possible that they also contribute to muscle identity in an active manner.

In *Drosophila*, the general framework for understanding muscle cell fusion was provided by Doberstein and colleagues (Doberstein et al., 1997) who subdivided the process into steps: cell-cell recognition, adhesion, alignment of membranes and membrane fusion. Genetic studies in *Drosophila* have also provided fusion mutants (Paululat et al., 1999). Essential loci for myoblast fusion include the transcriptional regulator Mef2 (Bour et al., 1995; Ranganayakulu et al., 1995), the membrane bound protein Rolling stones (Paululat et al., 1997), cytoplasmic proteins such as Blown fuse (Doberstein et al., 1997), and components of the Rac1 signaling pathway such as Myoblast city (Erickson et al., 1997; Nolan et al., 1998) and Drac1 (Luo et al., 1994). Interestingly, overexpression of weak gain-of-function Notch constructs throughout the mesoderm can completely block fusion without interfering with earlier roles for Notch (Fuerstenberg and Giniger, 1998) suggesting that Notch is also involved in muscle morphogenesis. Another family of proteins that plays crucial roles in myoblast fusion in *Drosophila* is the immunoglobulin (Ig) superfamily (Taylor, 2000; Frasch and Leptin, 2000; Baylies and Michelson, 2001). These Ig-containing proteins include Kirre (formerly Dumbfounded) (Ruiz-Gómez et al., 2000) and Sns (Bour et al., 2000). Although the described mutant phenotypes for *kirre* and *sns* are the same – a complete fusion block – their expression patterns in the somatic mesoderm are strikingly different. *kirre* is expressed exclusively in founder cells, while *Sns* is expressed exclusively in fusion-competent cells. Moreover, *kirre* is expressed during the entire fusion process and acts as an attractant for myoblasts, indicating that founder cells actively recruit fusion-competent cells until the final muscle size is achieved (Ruiz-Gómez et al., 2000). *Sns*, however, is a general marker for fusion-competent cells and, consistent with the segregation of these myoblasts, its expression depends on Notch signaling (Bour et al., 2000). Both *Kirre* and *Sns* are involved in the initial steps of myoblast cell-cell recognition as free myoblasts in embryos mutant for either gene do not cluster around founder cell, suggesting that there is no recognition between both types of myoblasts.

To study muscle identity and morphogenesis, we have devised a molecular screen to identify mRNAs that are expressed in founder or fusion-competent myoblasts (R. D. A. and M. K. B., unpublished). From this screen we isolated *hibris* (*hbs*), a novel gene that we have characterized molecular and genetically. We show that *hbs* is a single pass transmembrane protein belonging to the Ig superfamily and is involved in muscle morphogenesis. Phenotypic analysis of *hbs* and genetic interactions with *sns* suggests that Hbs is a dose-dependent regulator of myoblast fusion. Hbs is also a novel target of Notch and Ras signaling. In addition, we present evidence to suggest that fusion-competent cells may not be a homogeneous population over the course of muscle development.

MATERIALS AND METHODS

Drosophila genetics

Oregon R was used as the wild-type strain. *Df(1)w^{67k30}* was obtained from M. Ruiz-Gomez (Ruiz-Gomez et al., 2000); *sns^{XB3}* from S. Abmayr (Bour et al., 2000); *N^{55el1}* (Kidd et al., 1983) and *UAS-N^{intra}* from T. Lieber; and *UAS-ras^{N17}*, *UAS-ras^{V12}* and *twi-GAL4*; *Dmef2-GAL4* from A. Michelson. All other fly stocks were obtained from Bloomington, Umea or Szeged Stock Centers. Mobilization of P elements was achieved using the stable source of transposase Δ2-3 (Robertson et al., 1988). P homing was as described elsewhere (Taillebourg and Dura, 1999). Several genetic strategies were employed to mutate *hbs* (R. D. A. and M. K. B., unpublished). Briefly, two deficiencies, *Df(2R)X28* and *Df(2R)X7*, were generated by reversion of the EP(2)2590 associated *white⁺* minigene after γ-ray mutagenesis. Molecular mapping of the proximal ends of these deficiencies showed that *hbs* was deleted in *Df(2R)X28* but not in *Df(2R)X7* (Fig. 1A). We then performed EMS mutagenesis and recovered putative *hbs* mutations that mapped inside *Df(2R)X28* but outside *Df(2R)X7*. We isolated seven *hbs* alleles, all showing a rough eye phenotype. For phenotypic studies, relevant stocks were balanced with *CyO P[w⁺wg^{en11}lacZ]* or *FM7 P[w⁺ftz-lacZ]*.

Differential display screen for genes affecting muscle development

The details of this screen will be published elsewhere (R. D. A. and M. K. B., unpublished). Briefly, we generated two sets of embryos: one expressing an activated form of Notch (*UAS-N^{intra}*), which leads to suppression of founder cell fate (Landgraf et al., 1999), another expressing an activated form of Ras (*UAS-ras^{V12}*), which leads to enhancement of founder cell fate (Carmena et al., 1998b), under the control of *twi-Gal4*. In addition, these overexpression experiments were carried out in a *Toll^{10b}* genetic background to reduce tissue complexity. This mutation leads to a constitutively active Toll receptor, which results in *twist* activation throughout the embryo (Leptin et al., 1992). Ectopic expression of Twist converts the majority of cells into mesoderm and subsequently somatic muscle. RNA from embryo collections aged 5 to 9 hours were processed for differential display using the Delta Differential Display kit (Clontech). Forty-one differentially displayed bands were selected for further study.

Molecular biology

An embryonic cDNA library (Kidd, 1992) was screened with probe P1/T9(1), which was recovered from the differential display gel (Fig. 1A), yielding partial cDNAs A (2.2 kb) and B (2.1 kb). We then screened a 0–22 hour cDNA library (Rubin et al., 2000) with cDNA A and detected 12 clones. Restriction analysis showed that five (D2, C6, C9, C1 and D1) were identical in size (4.7 kb). cDNA D1 was sequenced and translated into a predicted protein (Fig. 1D). The beginning of the transcription unit was confirmed using the FirstChoice RLM-RACE kit (Cat. No. 1700, Ambion). RNA was extracted from appropriate samples using Tri-Reagent (Cat. No. T9424, Sigma) and poly A⁺ RNA purified with Oligotex mRNA spin-columns from Qiagen (Cat. No. 70042). Northern blots were processed according to the manufacturer recommendations for use of DIG-labeled probes (Roche Molecular Biochemicals). DNAs were sequenced at the Cornell University DNA sequencing facility (Ithaca, NY). Protein sequence analysis was carried out using the ExPASy (Expert Protein Analysis System) proteomics server from the Swiss Institute of Bioinformatics (Appel et al., 1994).

Germline transformation and constructs

Hbs protein was ectopically expressed using the UAS/GAL4 system (Brand and Perrimon, 1993). The full-length *hbs* construct (*UAS-hbs^{FL}*) was made by subcloning cDNA D1 into pUAST. Two additional constructs were made: *UAS-hbs^{ΔICD}*, which lacked the last 143 amino acids of the intracellular portion of the protein, and *UAS-*

hbs^{ΔECD}, which lacked 938 amino acids of the extracellular domain but retained the transmembrane region (see Fig. 7Q). *UAS-hbs*^{ΔECD} was created by deleting a 2.8 kb long *EagI/EcoRV* fragment from cDNA D1 and blunt end religation. The resulting plasmid, retaining the wild-type 5'UTR and signal peptide, was sequenced to verify the ORF. *UAS-hbs*^{ΔECD} was made by purifying a 4 kb *EcoRI/EcHKL* fragment from cDNA D1 that was blunted and ligated to a pBluescript plasmid containing the 3' UTR region from D1. The 3' UTR region from cDNA D1 was subcloned into pBluescript by using specific primers containing *Bam*HI and *Xho*I restriction sites. All constructs were recloned into pUAST and injected into *yw* embryos according to published procedures (Spradling and Rubin, 1982). For ectopic Hbs expression, flies containing the indicated *UAS-hbs* transgene were mated to GAL4 lines at 25°C or 29°C. For P homing, P[w⁺]36.1 was created using a PCR-amplified 4 kb fragment upstream the transcription unit (primers CAAGGCATTTCGCAGAAC and GTGTAGGCGGTTTCGTAGTC) cloned into a blunted *NotI* site in pETWnucLacZ. P element insertions in *hbs* were screened by PCR using primers specific for the transposable element and genomic primers.

Immunohistochemistry

The Hbs antibody was raised against a synthetic 15-mer peptide (1151-1165 in Hbs protein) supplied by Genossys. The peptide was made antigenic by coupling to the carrier tuberculin PPD (Statens Serum Institut, Denmark) using glutaraldehyde. This antigenic Hbs peptide was injected into rabbits at Pocono Rabbit Farm and Laboratory (Canandensis, PA), according to standard peptide-antigen protocols. Immunocytochemistry in embryos (Rushton et al., 1995) was performed using anti-Heavy Chain Myosin (1:1000; Kiehart and Feghali, 1986), anti-β-galactosidase (1:2000; Promega), anti-Fasciclin III (1:100; Developmental Studies Hybridoma Bank, University of Iowa) (Patel et al., 1987) and anti-Krüppel (1:2000; provided by J. Reintz). Hbs (1:3000) and Sns (1:100; Bour et al., 2000) antibodies were used preabsorbed against fixed wild-type embryos in combination with the TSA system from NEN (Cat. No. NEL700A) and a hot fixation protocol (Rothwell and Sullivan, 2000). Biotinylated secondary antibodies were used in combination with Vector Elite ABC kit (Vector Laboratories, CA). Immunofluorescent signals in co-localization studies were analyzed using a Leica TCS-NT confocal microscope. *hbs* RNA localization was detected using digoxigenin-labeled RNA probes, as described (O'Neil and Bier, 1994).

RESULTS

Identification of *hbs*

To better understand muscle diversity and morphogenesis, we devised a differential display screen to identify genes specifically expressed in founder versus fusion-competent myoblasts (R. D. A. and M. K. B., unpublished; Materials and Methods). In short, we made use of the observation that muscle progenitor specification depends on Notch and Ras signaling to repress or enhance muscle progenitor fate respectively (Carmena et al., 1998b; Landgraf et al., 1999). We overexpressed activated forms of Notch and Ras in *Toll*^{10b} mutant embryos (Leptin et al., 1992) to reduce tissue complexity. We have confirmed that *Toll*^{10b} mutant embryos differentiate almost exclusively as somatic mesoderm.

A differentially displayed band, P1/T9(1) (Fig. 1A), was chosen for further study because it was strongly upregulated under the activated Notch conditions. Corresponding cDNAs were isolated and the gene named *hbs* (Materials and Methods). We have confirmed *hbs* dependence on Notch by

Northern blot analysis. Fig. 1B compares *hbs* expression in *Toll*^{10b} mutant embryos and *Toll*^{10b} mutant embryos that expressed activated Ras or activated Notch. Our quantification of these Northern blot signals suggested that *hbs* expression was upregulated at least twofold upon Notch activation, and repressed at least fivefold upon Ras activation.

In a developmental Northern blot, we detected a *hbs* transcript of 6.2 kb with high levels of expression at mid-embryogenesis (Fig. 1C). We sequenced several cDNAs that had a 1235 amino acid ORF. *hbs* encoded a single pass transmembrane protein belonging to the Ig superfamily and contained nine Ig-C2 type repeats and a Fibronectin type III domain adjacent to its transmembrane region (Fig. 1D). A potential signal peptide sequence that is characteristic of membrane-bound proteins was present in the N terminus. BLAST database searches (Altschul et al., 1990) with Hbs revealed Nephlin as the human ortholog (29% identity, 44% similarity). Mutations in Nephlin have been linked to the Congenital Nephrotic Syndrome of the Finnish type (Kestilä et al., 1998). Furthermore, there was a *Drosophila* paralog, the protein Sns, with 48% identity and 63% similarity to Hbs (compare with Fig. 4 in Bour et al. (Bour et al., 2000)). The Hbs cytoplasmic domain, however, was shorter than its equivalent region in Sns (166 versus 376 amino acids, respectively). The Hbs extracellular region contained 13 NXS/T consensus triplets for N-glycosylation, eight of which were conserved in Sns. The cytoplasmic domain of the protein showed potential target sites for cAMP and cGMP-dependent protein kinases, protein kinase C (PKC), and casein kinase II (CKII). These phosphorylation sites were not conserved in Sns, except for a CKII site and a PKC site in two regions of strong conservation (Fig. 1E). In addition, Bour et al., reported conservation of tyrosine residues between Sns and Nephlin in the intracellular domain (Bour et al., 2000), which are also present in Hbs. The Hbs cytoplasmic domain also contained an eight amino acid direct repeat, but no described conserved domains. Additional searches against the conceptual translation of predicted genes in the *Drosophila* genome with the intracellular region of Hbs did not find any significant match except with Sns.

Pattern of *hbs* expression

hbs expression was analyzed by in situ hybridization in embryos (Fig. 2A-F) and in imaginal discs (not shown). We first detected *hbs* transcripts at stage 8 (Campos-Ortega and Hartenstein, 1985) in precursors of the amnioserosa and in the mesectoderm, where it was maintained in progeny of these midline cells throughout embryogenesis. By stage 10, *hbs* was expressed in the visceral mesoderm in a pattern reminiscent of *bagpipe*. These cells maintained *hbs* expression while forming the visceral mesoderm surrounding the gut (Fig. 2B,C). By late stage 11, *hbs* was expressed in somatic mesoderm (Fig. 2D) where its expression peaked between stage 12 and early stage 13, and subsequently declined, disappearing by stage 14. By stage 12 there was expression in the precursors of the heart, where *hbs* was maintained throughout the remainder of embryogenesis. Late *hbs* expression (Fig. 2F) was detected in the epidermis at putative muscle attachment sites, hindgut and pharyngeal muscles. *hbs* was also expressed in imaginal tissues, most notably in the eye-antennal, wing, leg and haltere discs (not shown).

Transgenic flies carrying a 4 kb fragment of *hbs* genomic sequence fused to a *lacZ* reporter (Materials and Methods)

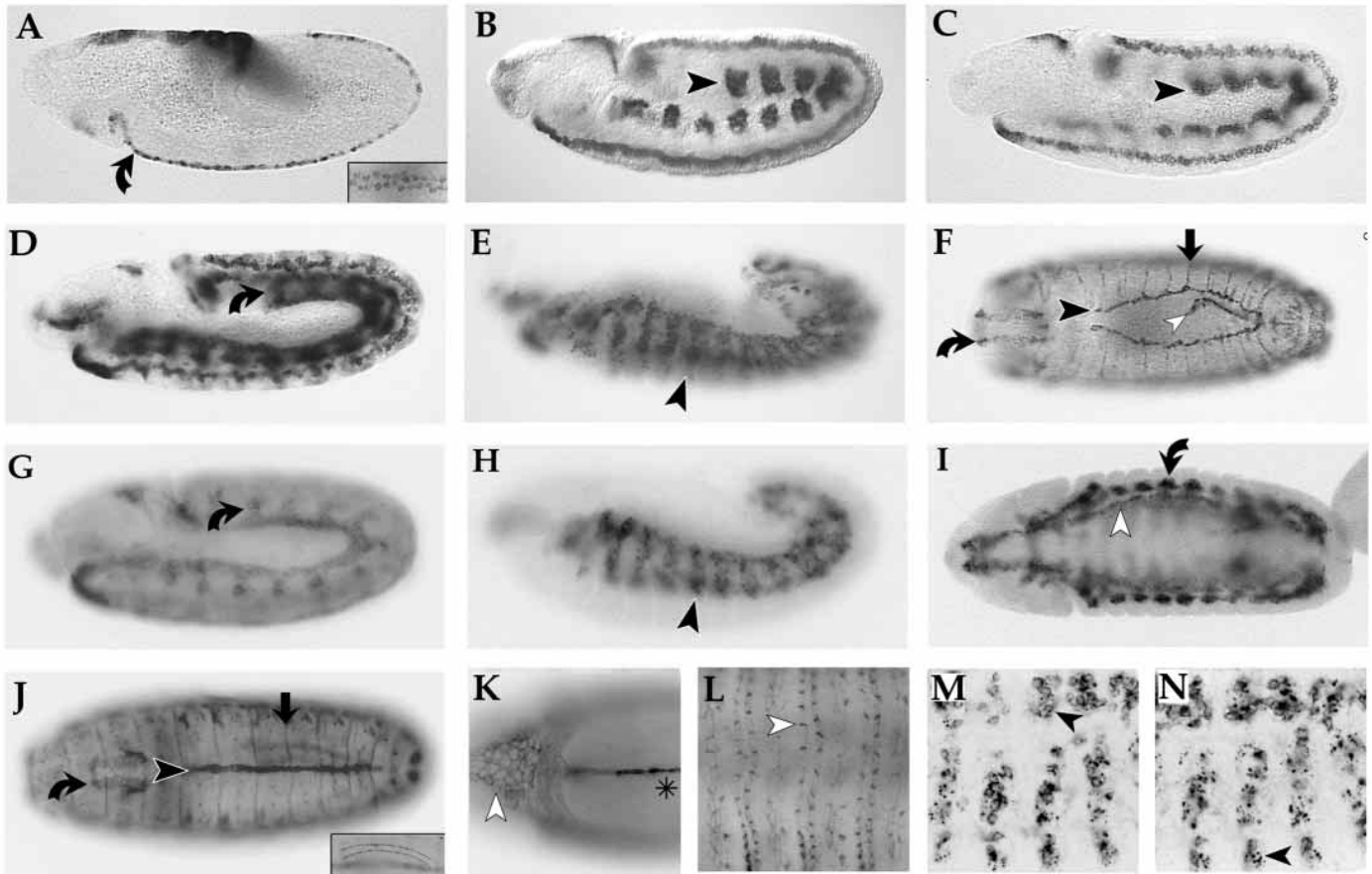


Fig. 2. Embryonic expression of *hbs* transcript and protein. In all panels anterior is towards the left and dorsal upwards. Lateral views (A-E,G,H,M,N), dorsal views (F,I,J) and ventral view (K). (A) *hbs* was first detected by stage 8 in the amnioserosa anlagen and in the mesectoderm (arrow). Inset shows a ventral view of the same embryo. Expression in the mesectoderm or its progeny remained throughout embryogenesis (see also B-D). (B,C) By early stage 10, transcription started in patches in precursors of the visceral musculature (B, arrowhead) where it continued to be expressed as these cells internalize (arrowhead, C). (D,E) Stage 11 embryo shows *hbs* expression in the somatic mesoderm (D, arrow). This expression increased as founder and fusion-competent cells fuse during germ band retraction (arrowhead, E). (F) The late expression pattern (stage 15) consisted of epidermal stripes at putative muscle attachment sites (straight arrow), heart precursors (black arrowhead), hindgut (white arrowhead) and pharyngeal muscles (bent arrow). (G-N) An anti-Hbs antibody reproduced the same pattern of expression and revealed finer details. (G) At stage 11 Hbs protein was detected in the dorsalmost part of the somatic mesoderm (arrow). (H,I) This expression was found throughout the somatic musculature by germ band retraction (arrowhead, H) and stage 13 (bent arrow, I). By this stage, Hbs was still detected in the visceral musculature (arrowhead, I). (J) By stage 16, Hbs was found in pharyngeal muscles (bent arrow), dorsal vessel (arrowhead) and epidermal attachment sites (straight arrow). (K-N) High magnification micrographs of several tissues show signal at cell border (arrowhead, K) and polarized expression of the protein. Hbs was restricted to the membranes in contact between mesectoderm cells (asterisk in germ band extended embryo K), to the luminal side of the hindgut (inset, J), to the contact side between cells at the epidermal attachments (arrowhead, L) and to discrete points at the myoblast membranes while fusion is in progress (arrowheads, M,N). I,N,M are confocal micrographs.

reproduced aspects of *hbs* expression and provided an additional tool with which to study *hbs*. Embryos containing this reporter inserted in the *hbs* locus (P[w⁺]36.1; Fig. 1A) showed expression in visceral and somatic mesoderm, mesectoderm, pharyngeal muscles and hindgut in a pattern similar to that found with the anti-Hbs antibody. To reinforce further that P[w⁺]36.1 recapitulated *hbs* expression in the mesoderm, we simultaneously detected β -galactosidase expression and *hbs* transcription in P[w⁺]36.1 embryos, confirming there was overlap between both signals (not shown). Because of the high degree of conservation between Hbs and the kidney protein Nephrin, we analyzed *hbs* expression in Malpighian tubules in our reporter P[w⁺]36.1. Interestingly, we detected weak expression at stage 12/13 in a

subset of tubule cells that, based on their morphology, appear to be stellate cells (not shown; H. Skaer, personal communication).

hbs is expressed in fusion-competent myoblasts

Fig. 1B establishes that *hbs* is regulated by Notch and Ras in a *Toll*^{10b} mutant background. We have confirmed this regulation in vivo in wild-type embryos. We studied *hbs* expression in Notch and Ras loss-of-function embryos and embryos overexpressing activated forms of Notch and Ras in the mesoderm (Fig. 3). A dominant negative Ras construct activated *hbs* expression in the somatic mesoderm. Zygotic null *Notch* embryos showed lower *hbs* transcription. Conversely, an activated form of Notch upregulated *hbs* in the mesoderm,

while an activated form of Ras almost completely inhibited *hbs* expression. These results argued that, upon stimulation, Notch activated *hbs*, while Ras acted as a negative signal, and predicted that *hbs* expression in the somatic mesoderm would be restricted to fusion-competent cells (Notch dependent) and excluded from founder cells (Ras dependent). We do not know whether this regulation is direct, that is, Notch or Ras effectors act directly on the *hbs* promoter, or indirect, that is, Notch/Ras converts cell fate, which in turn would lead to *hbs* upregulation/downregulation by some other effector.

As these results suggested that *hbs* was excluded from founder cells and was present in fusion-competent cells, we performed several additional experiments to confirm this possibility. Co-localization experiments using either P[w⁺]36.1 that reiterated Hbs expression in the mesoderm or Hbs antibody and various founder cell markers revealed that Hbs was absent from founder cells. These experiments also suggested that Hbs was not expressed in all fusion-competent cells during myoblast fusion (Fig. 4M-O; data not shown). Therefore, we asked whether Hbs and Sns, a protein known to be expressed exclusively in fusion-competent cells (Bour et al., 2000), co-localize in fusion-competent cells. Wild-type embryos double labeled with antisera against Sns and Hbs showed several examples of co-localization of these proteins. During stage 11, when muscle progenitors are being specified and the fusion process has not begun, Hbs expression was initially more widespread in somatic and visceral mesoderm than that of Sns (Fig. 4A-C). Subsequently, as the process of muscle fusion begins, Hbs expression was less widespread than Sns. We note that at this stage, although we detected overlap in Hbs and Sns expression, we found cases of Sns and Hbs-specific expression (Fig. 4D-F). At later stages of the fusion process, we no longer detected Hbs protein in the remaining fusion-competent cells, in contrast to the continued presence of Sns (Fig. 4G-I). We also found co-localization of both Hbs and Sns in the visceral mesoderm (Fig. 4J-L). We conclude that Hbs expression initially precedes Sns, but then largely overlaps with Sns, suggesting that Hbs could modulate the fusion-promoting properties of Sns in fusion-competent cells during the course of myoblast fusion.

Isolation of *hbs*-specific mutations

To assay the effects of loss of *hbs* function, we generated both new deficiencies around region 51D7 and EMS-induced mutations (Fig. 1A; Materials and Methods). For two of the EMS-induced mutations recovered, 2593 and 459 (hereafter *hbs*²⁵⁹³ and *hbs*⁴⁵⁹), we identified nucleotide changes in the *hbs* transcription unit, therefore establishing that they were *hbs* alleles. *hbs*²⁵⁹³ mutation was a T to A transversion in the second nucleotide of the intron between exons 9 and 10 (Fig. 5A). The mutation leads to an aberrantly spliced transcript that retained the whole intron and would result in a prematurely truncated protein. *hbs*⁴⁵⁹ was an A to T transversion in exon 7 that generated a stop codon (Fig. 5B).

Immunohistochemistry provided further confirmation that these mutations led to loss of *hbs* function. In these experiments, *hbs*²⁵⁹³ embryos showed a dramatic decrease in

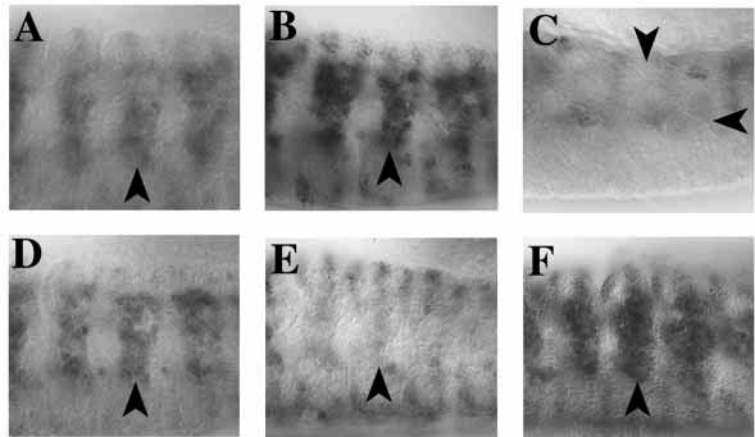


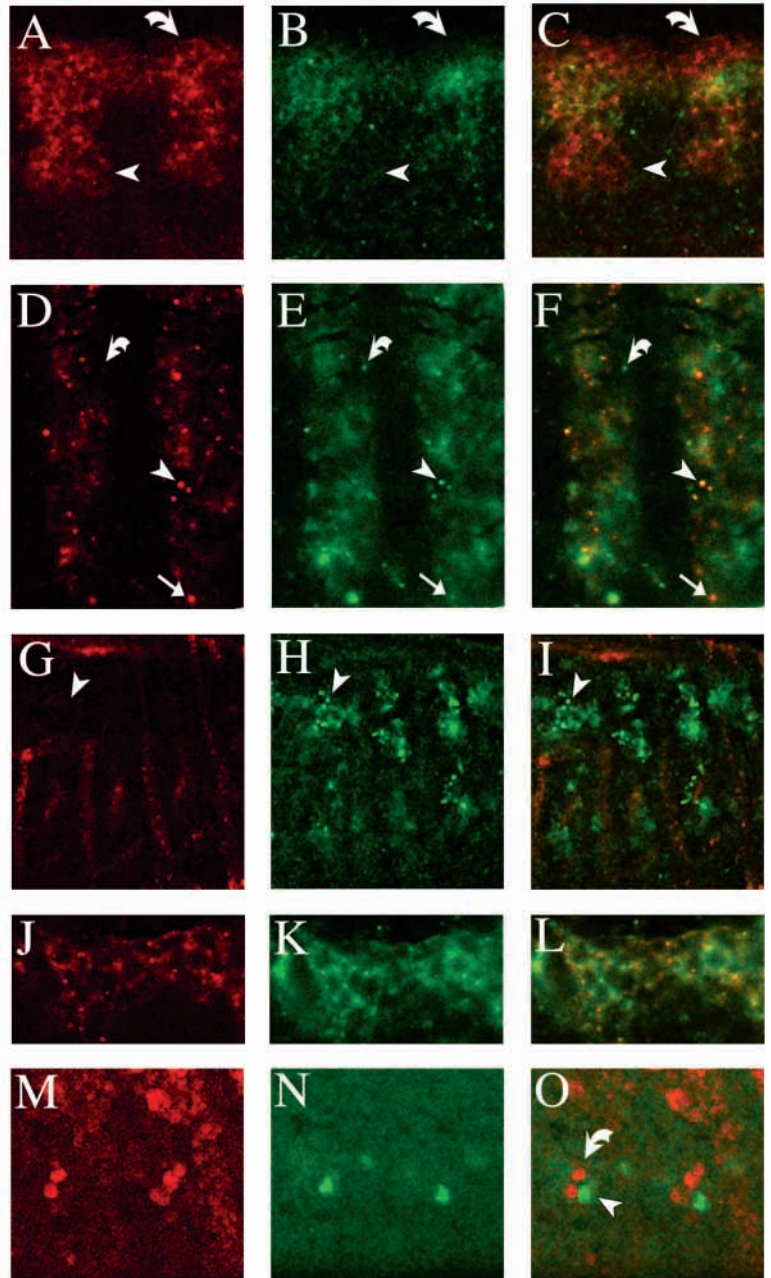
Fig. 3. *hbs* is a Notch and Ras signaling pathway target in vivo. *hbs* transcription detected in situ in wild-type embryos (A,D), zygotically null *N^{55e11}* (C), *twist-GAL4* driving dominant negative Ras (*UAS-ras1^{N17}*; B), activated Ras (*UAS-ras1^{V12}*; E) or activated Notch (*UAS-Nintra*; F). All pictures are lateral views at mid stage 12 showing segments T2-A2. Embryos A-C and D-F were hybridized in parallel experiments. Ras signaling represses (vertical arrowheads point to somatic mesoderm; compare A,B and D,E) while Notch signaling activates *hbs* transcription (compare A,C and D,F). Note CNS hyperplasia (horizontal arrowhead indicates lateral edge of the CNS) and lack of staining in the somatic mesoderm (vertical arrowhead) in C.

Hbs (Fig. 5C,E), while *hbs*⁴⁵⁹ homozygous embryos showed no detectable protein (Fig. 5D,F). Allele *hbs*³⁶¹ showed protein expression at levels indistinguishable from wild type (not shown) but behaved at least as strongly as *hbs*⁴⁵⁹ in our phenotypic assays.

hbs mutant embryos show a partial block in myoblast fusion and visceral mesoderm defects

Although *hbs* mutant flies survive to adult stages in normal numbers and show visible phenotypes such as rough eyes, reduced viability and semisterility (R. D. A. and M. K. B., unpublished), we also found clear abnormalities in muscle development in mutant embryos. Embryos heterozygous for *hbs*⁴⁵⁹/*Df(2R)X28*, and different *hbs* transallelic combinations, were probed with anti Myosin antibody and compared with their wild-type counterparts. In embryos lacking *hbs* function (Fig. 6), we found that the muscle pattern was specified, although some muscles were occasionally missing or showed abnormal morphologies (e.g. looked thinner than normal or had fewer nuclei than normal). Immunocytochemistry with antibodies directed against founder cell markers such as Krüppel, Even-skipped and Runt revealed a normal pattern (not shown). These embryos, however, reproducibly showed a partial fusion block: an increased number of free myoblasts were present when compared with wild-type embryos. We detected unfused myoblasts scattered around the muscles, surrounding the gut, heart and CNS (Fig. 6C,D). These free myoblasts showed extended processes, indicative of their competence to scan for founder cells. In these experiments, we studied stage 16 embryos to ensure that free myoblasts had the chance to fuse and that in this mutant background they failed to do so. Note, however, that by this developmental stage many unfused myoblasts might have undergone apoptosis, been phagocytosed and lost Myosin expression, decreasing the

Fig. 4. Hbs co-localizes with Sns at distinct points in the cell membrane of fusion-competent and visceral mesoderm myoblasts. Expression of Hbs (A,D,G,J in red) and Sns (B,E,H,K in green) was analyzed by immunofluorescence with confocal microscopy (A-L). Co-localization was assessed in images combining both channels (C,F,I,L) by presence of the yellow color. All panels are lateral views showing expression in somatic (A-I) or visceral mesoderm (J-L). Late stage 11 embryos (A,C) showed stronger and more widespread Hbs expression in somatic (arrowhead) and visceral mesoderm (arrow) than Sns. Both signals overlapped at the myoblast cell membrane (yellow in C). Late stage 12 embryos (D-F) showed characteristically punctate expression for both proteins, with yellow spots (arrowhead, F) indicating co-localization. Note that some foci of expression appeared to be Hbs (straight arrow) or Sns (bent arrow) specific. Stage 15 embryos (G-I) no longer express Hbs (G, arrowhead) but do express Sns (arrowheads, H,I) in putative unfused myoblasts. Stage 12 embryos (J-L) showed co-expression of Hbs and Sns in precursors of visceral mesoderm. (M-O) P[w⁺]36.1 embryos analyzed for co-expression of the *hbs* enhancer trap (in red) and Krüppel founder cell marker (in green). Ventrolateral views of mid-stage 12 embryos showed β -galactosidase expression (bent arrow, O) adjacent to a Krüppel-positive cell (arrowhead, O). No other mesodermal β -galactosidase-expressing nuclei could be seen above or below the indicated cluster, suggesting that this reporter was expressed in a subset of fusion-competent cells.



apparent number of unfused myoblasts (Bour et al., 1995). Loss of *hbs* function also interfered with the normal gut development as shown both by an enlargement of the first chamber (Fig. 6E-H) as well as by loss of visceral muscle progenitors at stage 12 (Fig. 6I,J).

***hbs* overexpression leads to a block in myoblast fusion and defects in visceral mesoderm**

We used the GAL4/UAS system (Brand and Perrimon, 1993) to assess the effect of *hbs* overexpression. When we expressed *UAS-hbs^{FL}* throughout the embryonic mesoderm driven by *twist-GAL4*; *DMef2-GAL4*, we detected defects both in the somatic and visceral mesoderm similar to loss of *hbs* function. In the somatic mesoderm, we found a partial fusion block with free myoblasts scattered at several locations (Fig. 7E,F). In addition, these embryos normally show a greater degree of muscle loss than *hbs* homozygous mutant embryos (Fig. 7A,B). Defects in the visceral mesoderm, as revealed by anti-Fasciclin III staining (Fig. 7M,N), were also found. Because delivering extra Hbs to both founder and fusion-competent myoblasts led to muscle losses, we tested whether all founder cells were correctly specified in these embryos. Antibody staining with the founder cell markers Krüppel, Even-skipped and Runt indicated that founder cells were correctly specified in embryos overexpressing Hbs (not shown). However, at later stages, we detected aberrant morphologies in the growing muscles (i.e. odd shapes; Fig. 7I,J), suggesting that prolonged Hbs expression was interfering with muscle morphogenesis rather than the initial specification.

To dissect which parts of the protein are important for

Hbs function, two additional constructs were tested. The constructs either deleted the extracellular (*UAS-hbs^{ΔECD}*) or the intracellular (*UAS-hbs^{ΔICD}*) region of the protein, but maintained the transmembrane domain such that the truncated proteins remain membrane anchored (Fig. 7Q). Overexpression of *UAS-hbs^{ΔECD}* in the mesoderm resulted in detectable phenotypes, indicating that the intracellular domain of Hbs alone can interfere with muscle development. Specifically, we detected a greater degree of fusion block and muscle loss as well as defects in the late pattern of founder cell markers compared with overexpression of the full-length Hbs (Fig. 7C,G,K). This construct also caused greater defects in visceral mesoderm, leading to a greater reduction of visceral muscle progenitors (Fig. 7O). Altogether, these results suggested that the cytoplasmic domain of Hbs is required for

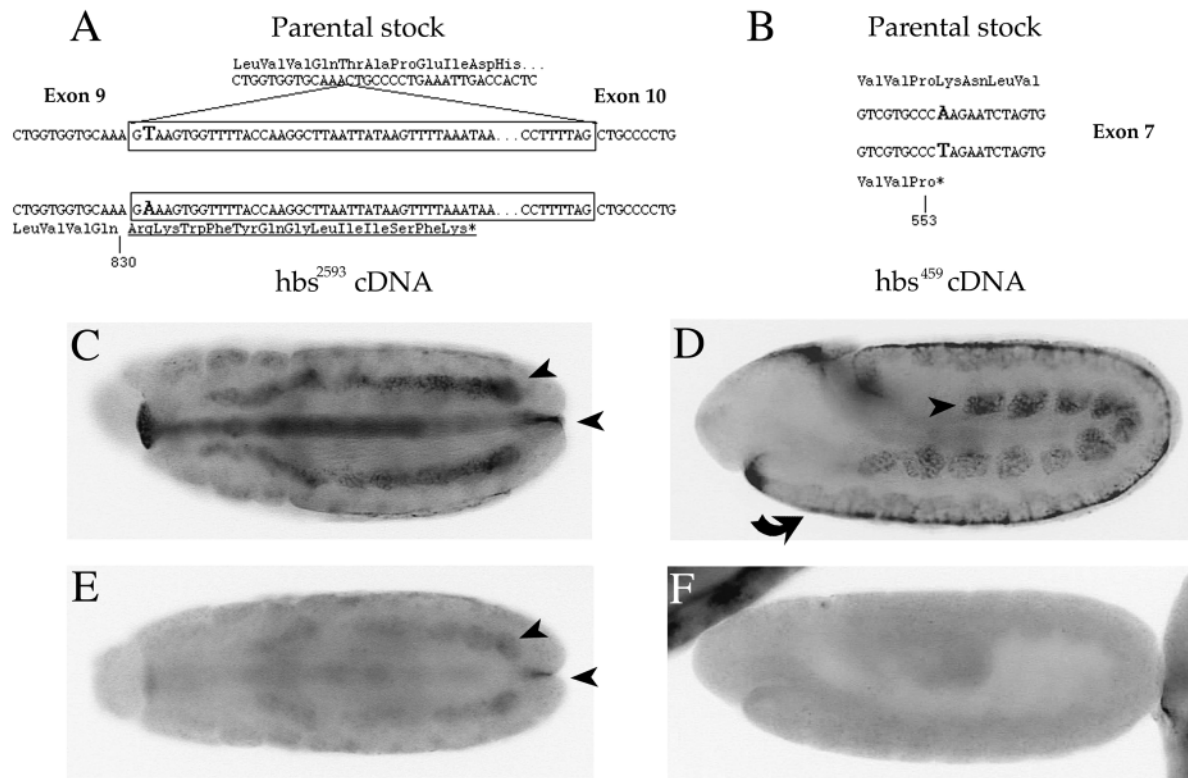


Fig. 5. Mutations mapped to the *hbs* transcription unit. (A) The donor/acceptor splice site nucleotide sequence (intron boxed) from the mutagenized stock is shown at the center. Wild-type splice event is shown above with its conceptual translation on top of the nucleotide sequence. cDNA clones from *hbs*²⁵⁹³ mutant flies showed a T to A transversion (large letters) in the donor splice site. The *hbs*²⁵⁹³ cDNA retained the intron between exon 9 and 10, apparently owing to mutation in the donor splice site. This, in turn, leads to a prematurely truncated protein as indicated by an asterisk. We detected a dramatic decrease in *hbs* immunoreactivity when comparing wild type (C) with *hbs*²⁵⁹³ homozygous mutant embryos (E). Note remaining expression in somatic mesoderm and midline (arrowheads) in C,E. (B) *hbs*⁴⁵⁹ was an A to T transversion at nucleotide 2029 in the cDNA sequence that leads to a non-sense codon and truncates the protein in position 553. (D) Antibody staining in wild-type embryos detected Hbs in visceral muscle precursors (arrowhead) and midline (bent arrow), while *hbs*⁴⁵⁹ homozygous mutant embryos showed a complete lack of Hbs (F).

hbs function in the mesoderm. By contrast, overexpression of *UAS-hbs*^{ΔCD} did not affect somatic muscle development appreciably but blocked visceral mesoderm development (Fig. 7D,H,L,P).

***hbs* interacts with *sns* in the somatic and visceral with mesoderm**

As *Sns*, *Kirre* and *Roughest* are all Ig-C2-containing proteins implicated in myoblast fusion (Bour et al., 2000; Ruiz-Gómez et al., 2000; Strunkelberg et al., 2001), we investigated their possible functional relationship with *hbs* by testing for genetic interactions. For this analysis we used first *Df(1)w*^{67k30}, which removes both *kirre* and *roughest*, both of which are suggested to be partially redundant in the fusion process (Strunkelberg et al., 2001). We found that *hbs* and *Df(1)w*^{67k30} did not interact genetically, either in loss- or gain-of-function *hbs* backgrounds (see Fig. 9I; data not shown). In addition, overexpression of *hbs* did not rescue any aspect of the *Df(1)w*^{67k30} phenotype (not shown) (Ruiz-Gómez et al., 2000).

As described above, Hbs and *Sns* co-localized at the cell membrane at discrete points, which would be consistent with both proteins working together in the fusion process. Figs 8, 9 show the result of manipulating the dose of *sns* and *hbs*. Stage 16 *hbs* homozygous mutant embryos characteristically showed

groups of free myoblasts throughout the embryo (Fig. 8D,G), and a gut phenotype revealed early by anti-Fasciclin III (Fig. 8F,I) or late by anti-Myosin staining (Fig. 8E,H). *hbs*-null embryos in which the *sns* dose was halved showed dominant suppression of both the partial fusion block and gut phenotype (Fig. 8J-L). When we analyzed *hbs* and *sns* double mutant embryos, we did not detect a noticeable change in the *sns* phenotype. Thus, *sns* and *hbs* appeared to act antagonistically.

Consistent with the hypothesis that *hbs* and *sns* act antagonistically rather than cooperatively in myoblast fusion, *sns* mutations dominantly enhance *hbs* overexpression phenotypes (Fig. 9). In the somatic muscles, there was an increase in the number of free myoblasts (Fig. 9C,E). This interaction also led to a greater loss in visceral muscle progenitors, as measured by Fasciclin III expression (Fig. 9D,F). To quantify these observations, we used the number of gaps in Fasciclin III expression in stage 12 embryos as a measurement of genetic interaction between *hbs* and *sns*. The result of this quantification was consistent with our qualitative analysis (Fig. 9I). We found that the dominant increase in Fasciclin III expression gaps when *sns* dose was lowered was statistically significant at the $P < 0.0001$ level, indicating that a synergistic, rather than an additive, effect between *hbs* overexpression and heterozygosity for *sns* accounts for the

increase in Fasciclin III expression gaps observed. As an additional test to determine the relationship between *hbs* and *sns*, we attempted to rescue the *sns* loss-of-function phenotype by overexpression of *hbs*. In this experiment, Hbs did not rescue the *sns* loss-of-function phenotype in the somatic muscles (not shown) in agreement with the genetic data presented above. Altogether, the results of these experiments suggested that *hbs* antagonizes *sns* function during mesoderm development, but cannot differentiate whether *sns* is downstream *hbs* or both genes are working in parallel pathways.

DISCUSSION

Hbs is an Ig domain protein involved in signal transduction

Hbs, Sns and Nephrin, in addition to their homologs in rat, mouse and *C. elegans*, establish a new subgroup in the Ig superfamily. These proteins show a characteristic run of 7-9 Ig-C2 domains in the extracellular domain followed by a single Fibronectin type III domain closest to the transmembrane region and no known motifs in their cytoplasmic tail. In agreement with the functions of the Ig superfamily, Hbs, Sns and Nephrin have been implicated in cell adhesion and/or cell signaling.

Clues to how Hbs functions during myogenesis have been revealed in our overexpression experiments. These data show that *hbs* overexpression gives a similar phenotype to *hbs* loss and suggest that either Hbs transduces a signal or our constructs behave as dominant negatives. In support of Hbs acting as a signal transducer, we find that overexpression of *UAS-hbs^{ΔECD}* resulted in a partial block in somatic muscle development, indicating that the cytoplasmic domain of Hbs mediates the activity of the protein. A similar dependence on the cytoplasmic domain of Notch in the embryonic nervous system (Lieber et al., 1993) or Echinoid in the eye imaginal discs (Bai et al., 2001) has been used as support for these proteins acting as signal transducers. Alternatively, our overexpression data with both the full-length and intracellular domain constructs could be interpreted as Hbs exerting a dominant negative effect through the titration of another crucial component, such as another membrane protein or cytoskeletal component. This key protein could be a target of Hbs without Hbs actually transducing a signal in the classical sense. However, as the behavior of mutant combinations of *sns* and *hbs* is different – Hbs loss of

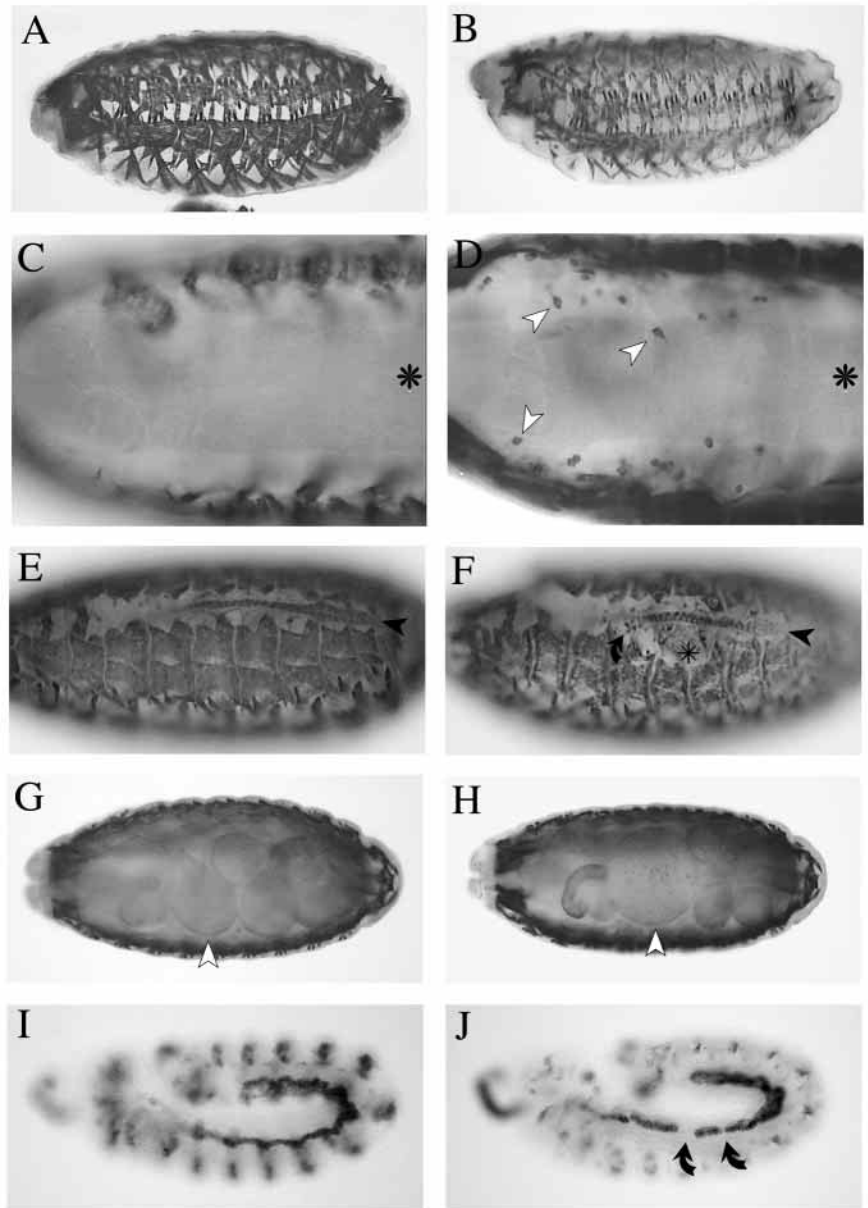


Fig. 6. *hbs* loss of function leads to a partial fusion block in somatic muscles and a visceral mesoderm phenotype. Wild-type (A,C,E,G,I) and *hbs⁴⁵⁹/Df(2R)X28* embryos (B,D,F,H,J) probed with anti-Myosin (A-H) or anti-Fasciclin III antibody (I,J). Anti-Myosin staining revealed that the overall pattern of somatic muscles was normal in *hbs*-null embryos (compare A with B). We detected a partial fusion block in embryos lacking *hbs* function as demonstrated by the presence of free myoblasts around the CNS (arrowheads, D) and around the heart (bent arrow, F). Note that unfused myoblasts can extend filopodia (arrowheads, D) suggesting that these free myoblasts can scan for founder cells but have failed to fuse. Asterisks indicate the CNS in C,D. *hbs* mutant embryos also showed a gut phenotype consisting of an enlarged first gut chamber (arrowheads, G,H), which pushes the dorsal muscles and heart up (black arrowheads in E,F). Asterisk in F denotes the gut. The gut phenotype may stem from an earlier reduction in the number of visceral mesoderm precursors, as suggested by the presence of gaps in embryos homozygous mutant for *hbs* (bent arrows, J)

function is suppressed by *sns* mutations whereas *hbs* overexpression is enhanced by *sns* mutations – we favor the possibility that Hbs transduces a signal rather than behaves as a dominant negative in the overexpression studies (Fig. 9). We

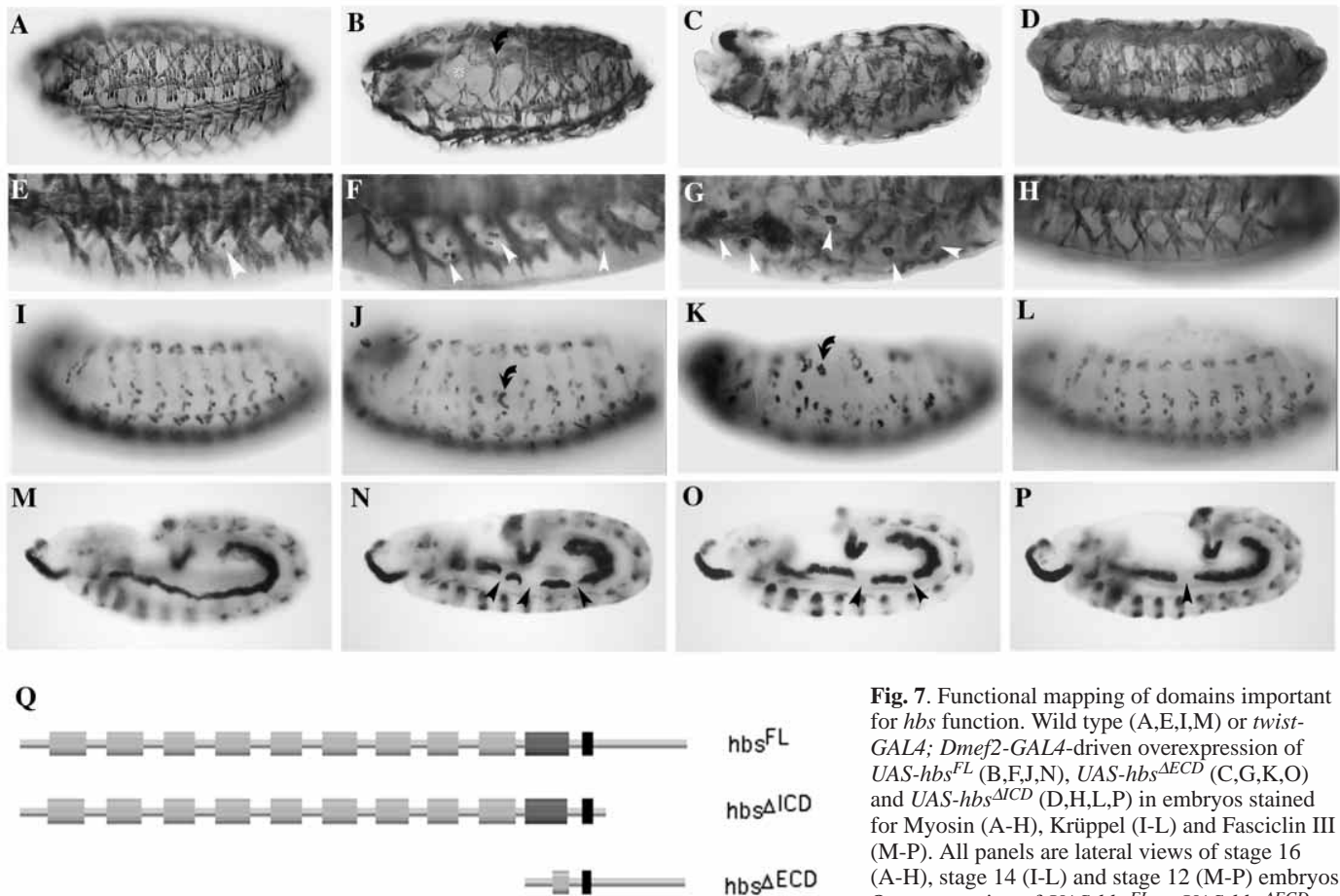


Fig. 7. Functional mapping of domains important for *hbs* function. Wild type (A,E,I,M) or *twist-GAL4; Dmef2-GAL4*-driven overexpression of *UAS-hbs^{FL}* (B,F,J,N), *UAS-hbs^{ΔECD}* (C,G,K,O) and *UAS-hbs^{ΔICD}* (D,H,L,P) in embryos stained for Myosin (A-H), Krüppel (I-L) and Fasciclin III (M-P). All panels are lateral views of stage 16 (A-H), stage 14 (I-L) and stage 12 (M-P) embryos. Overexpression of *UAS-hbs^{FL}* or *UAS-hbs^{ΔECD}* constructs throughout the mesoderm resulted in

partial fusion block (arrowheads, E-G) and muscle losses (white asterisk, B; note also losses in C). Bent arrow in B indicates dorsal muscles that are abnormally fused together. Specification of the founder cell marker Krüppel was normal initially yet later showed an abnormal pattern (I-K). Bent arrows in J,K designate LT and DA1/DO1 muscle precursors showing an abnormal morphology, respectively. By contrast, *UAS-hbs^{ΔICD}* overexpression in forming somatic muscles did not appreciably interfere with myogenesis (D,H,L). Overexpression of either *UAS-hbs^{FL}*, *UAS-hbs^{ΔECD}* or *UAS-hbs^{ΔICD}* constructs in the visceral mesoderm resulted in defects in Fasciclin III expression (arrowheads), suggesting abnormal segregation of visceral mesoderm precursors (M-P). (Q) Schematic representation of the constructs used in this study. *UAS-hbs^{FL}* is a full-length *hbs* protein, *UAS-hbs^{ΔICD}* is a 1093 amino acid long version that lacks the cytoplasmic region, and *UAS-hbs^{ΔECD}* is a 277 amino acid long construct deleting the extracellular domain of the protein. Light gray boxes represent Ig-C2 domains, dark gray boxes represent Fibronectin type III domains and black boxes represent the transmembrane region.

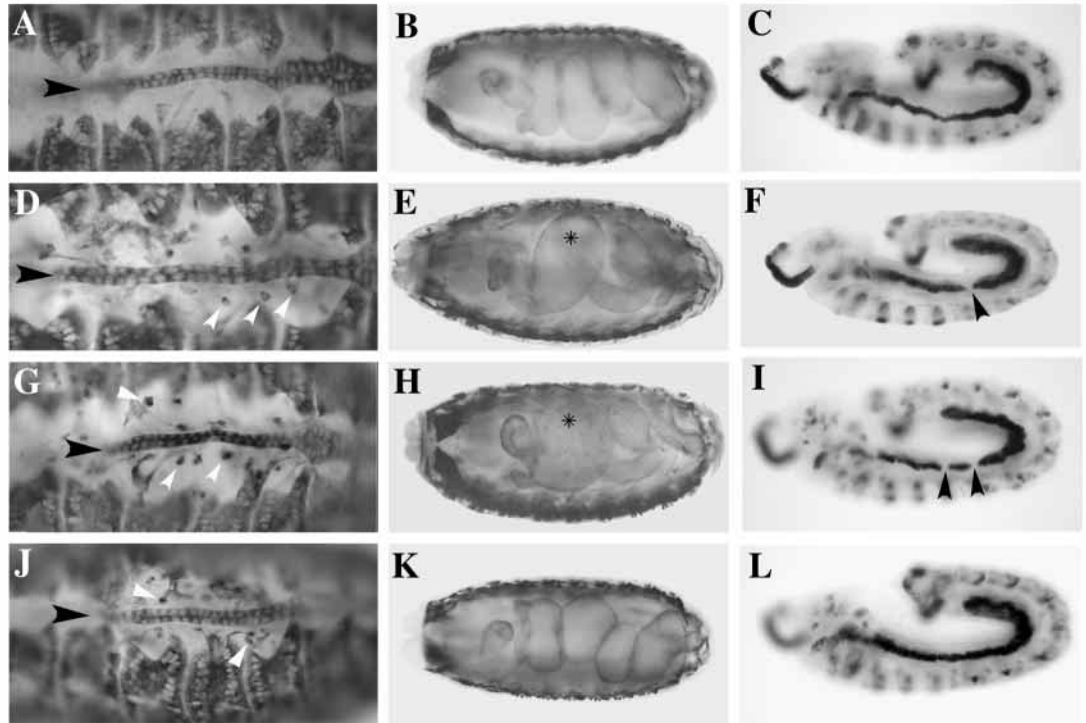
would expect *sns* heterozygosity to suppress both the *hbs* loss and overexpression phenotypes if *hbs* overexpression was acting as a dominant negative. Our data also indicate that the extracellular domain of *hbs* does not behave as a dominant negative construct either, at least in the somatic mesoderm, because overexpression of this construct does not cause a detectable phenotype in the somatic musculature (Fig. 7D,H,L).

Given the lack of enzymatic features in the cytoplasmic domain, we propose that Hbs associates with adapter proteins to connect to the cytoskeleton, cytoplasmic kinases or other transmembrane receptors. Interestingly, the intracellular domain contains motifs that are conserved in *Sns*. These motifs could potentially serve as interfaces for adaptor proteins. Work with Nephlin provides a putative candidate, the mouse CD2-associated protein (CD2AP). CD2AP, an SH3-containing cytoplasmic protein, has been shown to interact with the intracellular domain of Nephlin and has been proposed to

anchor Nephlin to the actin cytoskeleton at the slit diaphragm in the kidney (Shih et al., 1999) and to participate in setting up the immunological synapse in T cells (Dustin et al., 1998). The *Drosophila* genome contains a CD2AP homolog, which is being analyzed in our laboratory.

Overexpression of *UAS-hbs^{ΔECD}* or *UAS-hbs^{FL}* throughout the mesoderm resulted in a partial fusion block, but with greater muscle loss and morphological defects when compared with the loss of function phenotype. This increased muscle loss could reflect that, in our overexpression experiments, we express Hbs in both fusion-competent as well as founder cells, thereby breaking the expression asymmetry that is found under normal situations. However, we could equally suppose that prolonged and higher levels of Hbs block muscle fusion and disrupt later events in muscle morphogenesis. We note that both loss and gain of *hbs* result in a fusion phenotype. Although it is obvious why gain of a negative regulator could result in a fusion block, it is less clear why loss results in a

Fig. 8. *hbs* antagonizes *sns* function during myoblast fusion and gut morphogenesis. Wild type (A-C) or embryos with genotypes *hbs*²⁵⁹³/*Df(2R)X28* (D-F), *hbs*⁴⁵⁹/*Df(2R)X28* (G-I) and *sns*^{XB3}/*hbs*²⁵⁹³/*hbs*⁴⁵⁹ (J-L) are shown. Heart (black arrowheads, A,D,G,J) and gut (B,E,H,K) views of stage 16 embryos stained for Myosin, and lateral views of stage 12 embryos stained for Fasciclin III (C,F,I,L). *hbs* homozygous mutant embryos showed not only a partial fusion block, particularly conspicuous around the heart (compare A with D,G white arrowheads), but also an aberrant morphology of the gut chambers (asterisks) in late embryos (compare B with E,H), and gaps in the visceral mesoderm (black arrowheads; compare C with F,I). Both aspects were suppressed by halving the *sns* genetic dose (compare D-F with J-L).



similar phenotype. We speculate that *hbs* highlights a novel aspect of the regulated events in the fusion process.

Ig-containing proteins as adhesion receptors in fusion

Cell recognition and adhesion between myoblasts is the first step of the fusion process (Doberstein et al., 1997). Kirre has been shown to be expressed in founder cells and behave as a myoblast attractant. By contrast, *Sns* is expressed in fusion competent myoblasts exclusively. A simple model can be proposed with these data: Kirre interacts at the cell surface with *Sns* to allow recognition between founder and fusion-competent cells (Taylor, 2000; Frasch and Leptin, 2000). Subsequently, this recognition would signal the start of an orderly fusion process that requires such proteins as Rac, Blown fuse and Rolling stone. Later, myotubes continue to 'grow' by this process of attraction, recognition and fusion in a directed manner, sending growth cone-like structures toward specific attachment sites (Bate, 1993). Our analysis suggests that Hbs acts at the first step of this process as free myoblasts in *hbs* mutant embryos do not cluster nearby muscles (like *sns*) (Bour et al., 2000). In addition, Hbs serves as a negative regulator of *Sns* activity. This negative regulation is necessary to complete the fusion process as in *hbs* mutant embryos we find unfused myoblasts.

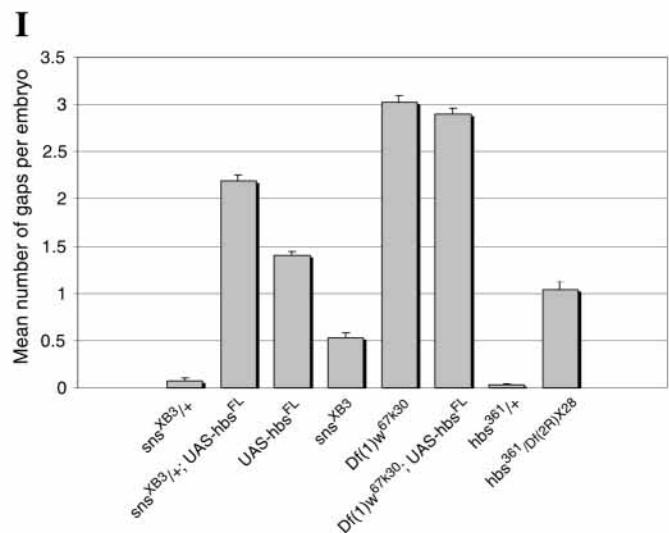
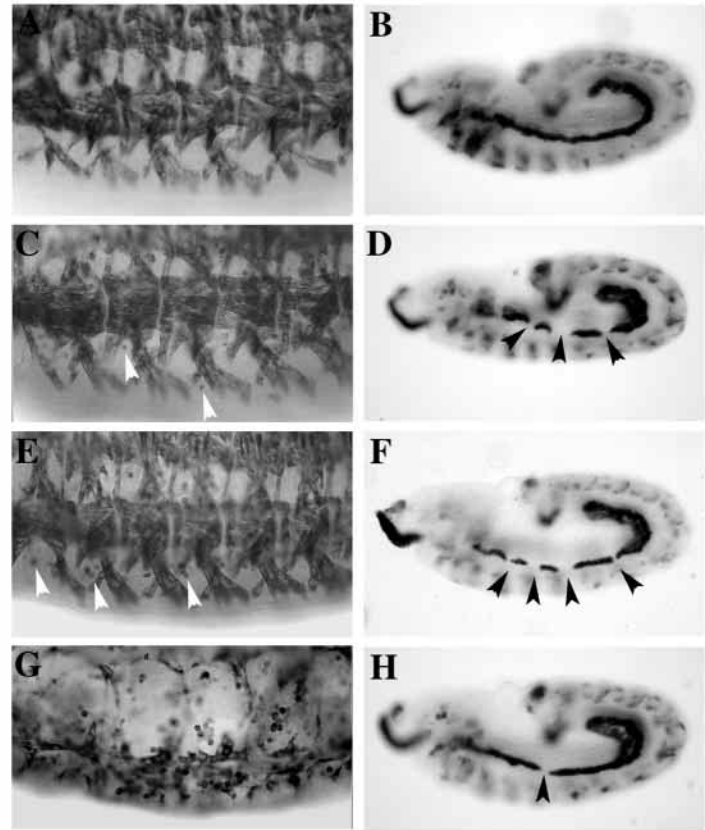
There are several ways in which Hbs could antagonize *Sns* function at the molecular level. Firstly, Hbs could compete for a putative *Sns* 'ligand'. Given the similarity (69%) of the extracellular domains of Hbs and *Sns*, this appears reasonable. However, we show that overexpression of the extracellular domain of Hbs alone can not block myoblast fusion, while the full-length construct does. Moreover, our data support a requirement for activity of the intracellular domain of Hbs.

Secondly, Hbs and *Sns* could form a receptor complex which switches the positive *Sns* signal to a negative signal. An example of this type of regulation is seen with the Netrin receptors, UNC-40/Deleted in Colorectal Cancer (DCC) and UNC-5 (Hong et al., 1999). Whereas axons expressing UNC-40/DCC are attracted to the ligand source positively, axons expressing both UNC-40/DCC and UNC-5 now are repelled and move away from the source of ligand. A third possibility would have Hbs and *Sns* function independently of one another but converge intracellularly on downstream proteins involved in fusion. For example Echinoid, an Ig domain protein resembling Hbs in overall structure, has been shown to antagonize the Ras pathway in the eye, not at the cell membrane but intracellularly at the level of transcription of a target gene, *tramtrack* (Bai et al., 2001). Hbs, *Sns* and Kirre may also be functioning together similarly in the generation of the visceral muscles, as recent data indicate that visceral muscles are not mononucleated, as previously reported, but syncytial (Klapper et al., 2001; San Martin et al., 2001).

Are all fusion-competent myoblasts functionally equivalent?

We find that Hbs and *Sns* co-localize at the cell membrane, which could correspond to focal adhesion points between founder cell and fusion-competent cells or among fusion competent myoblasts. However, Hbs precedes *Sns* temporally in the somatic and visceral mesoderm at stage 11, prior to the initiation of fusion. The two expression patterns largely overlap during stage 12-13 as fusion begins, with some *Sns* and Hbs-specific foci of expression, and by late stage 14 unfused myoblasts are basically devoid of Hbs but maintain *Sns* as fusion continues towards completion. We note that these differences in the pattern of expression of *Sns* and Hbs are

Fig. 9. *hbs* overexpression phenotype is sensitive to the *sns* genetic dose. Ventrolateral views of stage 16 embryos stained with anti-Myosin (A,C,E,G) and lateral views of stage 12 embryos stained with anti-Fasciclin III (B,D,F,H) antibody. Wild-type embryos (A,B) and embryos overexpressing *UAS-hbs^{FL}* under the control of *twist-GAL4*; *Dmef2-GAL4* in a wild-type background (C,D), or *sns^{XB3}* heterozygous background (E,F). *sns^{XB3}* homozygous embryos (G,H) are shown as control. *Hbs* overexpression throughout the mesoderm leads to an increase in the number of free myoblasts (arrowheads, C) and abnormalities in early stages of visceral mesoderm development (arrowheads, D). This phenotype was dominantly enhanced by *sns*. Note increased numbers of free myoblasts (arrowheads, E; compare with C) and presence of more defects in the visceral mesoderm (arrowheads, F; compare with D). *sns* mutant embryos showed complete myoblast fusion block (G) and a weak visceral mesoderm phenotype (arrowhead, H). (I) Representation of mean number of Fasciclin III expression gaps per embryo at mid-stage 12 in the indicated genotypes. Bars designate standard error. Fasciclin III expression gap phenotype caused by overexpression of *hbs* was dominantly enhanced by lowering *sns* dose (compare *UAS-hbs^{FL}* with *sns^{XB3}/+*; *UAS-hbs^{FL}* values). This increase was statistically significant at $P < 0.0001$ (Student's *t*-test). A deficiency that removed *kirre* and *roughest*, *Df(1)w67k30*, did not appreciably modify the *hbs* overexpression phenotype in the visceral mesoderm. Note also presence of Fasciclin III expression gaps in embryos homozygous for *sns^{XB3}* (0.53 per embryo) and *hbs* (1.04 per embryo).



meaningful as, when we genetically remove *hbs* such that fusion competent cells express *Sns* exclusively, we detect a muscle fusion phenotype. *Hbs* could, therefore, be revealing different potentials for the fusion-competent cells during muscle formation. Initially, cells that fail to become muscle progenitors during the first round of segregation (e.g. C2/P2 segregation) (Carmena et al., 1995) may be included in a new equipotential cluster. These clusters appear largely to overlap and form in rapid sequence. Early *Hbs* expression could participate in maintaining myoblasts that fail to become progenitors in the first round of selection uncommitted for successive rounds of progenitor segregation. This provides a reasonable explanation for occasional muscle losses in *hbs* mutant embryos. Subsequently, upon adoption of fusion-competent cell fate and expression of *Sns*, *Hbs* could regulate early events in fusion, maintaining an orderly process. During later events in the fusion process (i.e. while myotubes are already growing towards their specific attachment sites), when there are fewer free fusion-competent cells, *Hbs* may no longer be necessary to regulate or orient fusion. We thus propose three 'fusion-competent cell' stages:

(1) Pre-fusion stage. Early somatic myoblasts respond first to a laterally inhibiting Notch signaling event by expressing *Hbs* and subsequently have another chance at progenitor cell fate.

(2) Early fusion stage. Once the progenitor developmental option passes, the *Hbs*-expressing cells opt for fusion-competent fate. Expression of both *Hbs* and *Sns* regulates early steps in recognition and fusion of founders to fusion competent cells.

(3) Late fusion stage. Fusion-competent cells no longer require *Hbs* expression but do require *Sns*.

As founder cell markers such as Krüppel and Even-skipped

define subsets of founders, we envisage that additional markers will be found that serve to characterize these different fusion-competent cell stages. Moreover, our *hbs* enhancer trap provides a novel tool to recognize subsets of fusion-competent cells without the technical difficulties associated with a punctate, membrane-bound signal.

Pleiotrophy of *Hbs* and links to Notch

Clearly, *Sns* is not the only potential partner for *Hbs*. Although *Sns* is expressed in the visceral mesoderm and muscle attachments, it is not expressed in heart, midline, hindgut, Malpighian tubules, imaginal discs or adult tissues where we

find *hbs* expression and phenotypes. Either Hbs is acting alone in these tissues or it is interacting with other Ig domain proteins. Similarly, Sns does not always act with Hbs. Sns, like Kirre, is expressed in garland cells, yet Hbs is not.

Although Hbs operates in multiple places, we do find one unifying theme to *hbs* pleiotropy – an association with Notch signaling. Our evidence demonstrates that *hbs* is a novel target of Notch activity in the somatic musculature. There are also several compelling similarities between the *hbs* and *Notch* activities over the course of development. Weak gain-of-function Notch constructs block myoblast fusion, one of the aspects of *hbs* phenotype (Fuerstenberg and Giniger, 1998). Notch is involved in planar polarity in the eye and both *hbs* loss- and gain-of-function lead to polarity defects (N. Paricio, personal communication). Preliminary results suggest that the *hbs* semisterility phenotype is due to failure to specify stalk cells in the ovarioles (N. Matova, personal communication), a phenotype described for *Notch* loss-of-function mutations. We also find that *hbs* overexpression in adults show misplacement of bristles and that *hbs* and *Notch* interact weakly in the wings, resulting in a measurable increase in wing nicks. Perhaps like the *Enhancer of split* complex, *hbs* could mediate part of Notch signaling. Future work will be directed to uncover the interaction between these two genes throughout development.

We thank the BDGP consortium for LD cDNA library; Bloomington and UMEA stock centers for fly strains; Patrick Morcillo and Kathryn Anderson for genetic advice; Lanre Adedokun, Jason Kass, Vidya Kishore, Maia Dorsett and Sabino Guzman for technical assistance; and H. Thaler for assistance with the statistical analysis. We thank A. Martinez-Arias, A. Michelson, M. Ruiz-Gomez, K. Anderson and members of our laboratory for comments on the manuscript. We also thank M. Chakravarti from S. Abmayr's laboratory for providing purified Sns antibody necessary to complete this work. The project described was made possible in part by funds granted by the Charles H. Revson Foundation to R. D. A., the Muscular Dystrophy Association, The Society of Memorial Sloan Kettering Cancer Center, The New York Academy of Science – Speaker's Fund for Biomedical Research Toward the Science of Patient Care and National Institutes of Health (GM 56989) to M. K. B.

REFERENCES

- Altschul, S. F., Gish, W., Miller, W., Myers, E. W. and Lipman, D. J. (1990). Basic local alignment search tool. *J. Mol. Biol.* **215**, 403-410.
- Appel, R. D., Bairoch, A. and Hochstrasser, D. F. (1994). A new generation of information retrieval tools for biologists: the example of the ExPASy WWW server. *Trends Biochem. Sci.* **19**, 258-260.
- Bai, J., Chiu, W., Wang, J., Tzeng, T., Perrimon, N. and Hsu, J. (2001). The cell adhesion molecule Echinoid defines a new pathway that antagonizes the *Drosophila* EGF receptor signaling pathway. *Development* **128**, 591-601.
- Bate, M. (1990). The embryonic development of larval muscles in *Drosophila*. *Development* **110**, 791-804.
- Bate, M. (1993). The mesoderm and its derivatives. In *The Development of Drosophila melanogaster*. Vol. II (ed. M. Bate and A. Martínez Arias), pp. 1013-1090. Cold Spring Harbor: Cold Spring Harbor Laboratory Press.
- Bate, M., Rushton, E. and Frasch, M. (1993). A dual requirement for neurogenic genes in *Drosophila* myogenesis. *Development Suppl.* 149-161.
- Baylies, M. and Michelson, A. (2001). Invertebrate myogenesis: looking back to the future of muscle development. *Curr. Opin. Genet. Dev.* **11**, 431-439.
- Bour, B. A., O'Brien, M. A., Lockwood, W. L., Goldstein, E., Bodmer, R., Taghert, P. H., Abmayr, S. M. and Nguyen, H. T. (1995). *Drosophila* MEF2, a transcription factor that is essential for myogenesis. *Genes Dev.* **9**, 730-741.
- Bour, B. A., Chakravarti, M., West, J. M. and Abmayr, S. M. (2000). *Drosophila* SNS, a member of the immunoglobulin superfamily that is essential for myoblast fusion. *Genes Dev.* **14**, 1498-1511.
- Brand, A. and Perrimon, N. (1993). Targeted gene expression as a means of altering cell fates and generating dominant phenotypes. *Development* **118**, 401-415.
- Buff, E., Carmena, A., Gisselbrecht, S., Jimenez, F. and Michelson, A. M. (1998). Signaling by the *Drosophila* epidermal growth factor receptor is required for the specification and diversification of embryonic muscle progenitors. *Development* **125**, 2075-2086.
- Campos-Ortega, J. A. and Hartenstein, V. (1985). *The Embryonic Development of Drosophila melanogaster*. Berlin: Springer Verlag.
- Carmena, A., Bate, M. and Jiménez, F. (1995). *lethal of scute*, a proneural gene, participates in the specification of muscle progenitors during *Drosophila* embryogenesis. *Genes Dev.* **9**, 2373-2383.
- Carmena, A., Gisselbrecht, S., Harrison, J., Jimenez, F. and Michelson, A. (1998a). Combinatorial signaling codes for the progressive determination of cell fates in the *Drosophila* embryonic mesoderm. *Genes Dev.* **15**, 3910-3922.
- Carmena, A., Murugasu-Oei, B., Menon, D., Jimenez, F. and Chia, W. (1998b). *inscuteable* and *numb* mediate asymmetric muscle progenitor cell divisions during *Drosophila* myogenesis. *Genes Dev.* **12**, 304-315.
- Corbin, V., Michelson, A. M., Abmayr, S. M., Neel, V., Alcamo, E., Maniatis, T. and Young, M. W. (1991). A role for the *Drosophila* neurogenic genes in mesoderm differentiation. *Cell* **67**, 311-323.
- Doberstein, S., Fetter, R., Mehta, A. and Goodman, C. (1997). Genetic analysis of myoblast fusion: *blown fuse* is required for progression beyond the prefusion complex. *J. Cell Biol.* **136**, 1249-1261.
- Dohrmann, C., Azpiazu, N. and Frasch, M. (1990). A new *Drosophila* homeo box gene is expressed in mesodermal precursor cells of distinct muscles during embryogenesis. *Genes Dev.* **4**, 2098-2111.
- Dustin, M., Olszowy, M., Holdorf, A., Li, J., Bromley, S., Desai, N., Widder, P., Rosenberger, F., Anton van der Merwe, P., Allen, P. and Shaw, A. (1998). A novel adaptor protein orchestrates receptor patterning and cytoskeletal polarity in T-cell contacts. *Cell* **94**, 667-677.
- Erickson, M. R. S., Galletta, B. J. and Abmayr, S. M. (1997). *Drosophila* myoblast city encodes a conserved protein that is essential for myoblast fusion, dorsal closure, and cytoskeletal organization. *J. Cell Biol.* **138**, 589-603.
- Frasch, M. (1999). Controls in patterning and diversification of somatic muscles during *Drosophila* embryogenesis. *Curr. Opin. Genet. Dev.* **9**, 522-529.
- Frasch, M. and Leptin, M. (2000). Mergers and acquisitions: unequal partnerships in *Drosophila* myoblast fusion. *Cell* **102**, 127-129.
- Fuerstenberg, S. and Giniger, E. (1998). Multiple roles for Notch in *Drosophila* myogenesis. *Dev. Biol.* **201**, 66-77.
- Halfon, M. S., Carmena, A., Gisselbrecht, S., Sackerson, C. M., Jimenez, F., Baylies, M. K. and Michelson, A. M. (2000). Ras pathway specificity is determined by the integration of multiple signal-activated and tissue-restricted transcription factors. *Cell* **103**, 63-74.
- Hong, K., Hinck, L., Nishiyama, M., Poo, M., Tessier-Lavigne, M. and Stein, E. (1999). A ligand-gated association between cytoplasmic domains of UNC5 and DCC family receptors converts netrin-induced growth cone attraction to repulsion. *Cell* **97**, 927-941.
- Kestilä, M., Lenkkeri, U., Männikkö, M., Lamerdin, J., McCready, P., Putaala, H., Ruotsalainen, V., Morita, T., Nissinen, M., Herva, R. et al. (1998). Positionally cloned gene for a novel glomerular protein – nephrin – is mutated in congenital nephrotic syndrome. *Mol. Cell* **1**, 575-582.
- Kidd, S. (1992). Characterization of the *Drosophila cactus* locus and analysis of interactions between cactus and dorsal proteins. *Cell* **71**, 623-635.
- Kidd, S., Lockett, T. and Young, M. (1983). The *Notch* locus of *Drosophila melanogaster*. *Cell* **34**, 421-433.
- Kiehart, D. P. and Feghali, R. (1986). Cytoplasmic myosin from *Drosophila melanogaster*. *J. Cell Biol.* **103**, 1517-1525.
- Klapper, R., Heuser, S., Strasser, T. and Janning, W. (2001). A new approach reveals syncytia within the visceral musculature of *Drosophila melanogaster*. *Development* **128**, 2517-2524.
- Landgraf, M., Baylies, M. and Bate, M. (1999). Muscle founder cells regulate defasciculation and targeting of motor axons in the *Drosophila* embryo. *Curr. Biol.* **9**, 589-592.
- Leptin, M., Casal, J., Grunewald, B. and Reuter, R. (1992). Mechanisms of early *Drosophila* mesoderm formation. *Development Suppl.* 23-31.
- Lieber, T., Kidd, S., Alcamo, E., Corbin, V. and Young, M. (1993).

- Antineurogenic phenotypes induced by truncated Notch proteins indicate a role in signal transduction and may point to a novel function for Notch in nuclei. *Genes Dev.* **7**, 1949-1965.
- Luo, L., Liao, J., Jan, L. Y. and Jan, Y. N.** (1994). Distinct morphogenetic functions of similar small GTPases: *Drosophila* Drac1 is involved in axonal outgrowth and myoblast fusion. *Genes Dev.* **8**, 1787-1802.
- Nolan, K., Barrett, K., Lu, Y., Hu, K., Vincent, S. and Settleman, J.** (1998). Myoblast city, the *Drosophila* homolog of DOCK180/CED-5, is required in a Rac signaling pathway utilized for multiple developmental processes. *Genes Dev.* **12**, 3337-3342.
- O'Neil, J. W. and Bier, E.** (1994). Double-label in situ hybridization using biotin, digoxigenin-tagged RNA probes. *Biotechniques* **17**, 870.
- Patel, N., Snow, P. and Goodman, C.** (1987). Characterization and cloning of Fasciclin III: A glycoprotein expressed on a subset of neurons and axon pathways in *Drosophila*. *Cell* **48**, 975-988.
- Paululat, A., Goubeaud, A., Damm, C., Knirr, S., Burchard, S. and Renkawitz-Pohl, R.** (1997). The mesodermal expression of *rolling stone* (*rost*) is essential for myoblast fusion in *Drosophila* and encodes a potential transmembrane protein. *J. Cell Biol.* **138**, 337-348.
- Paululat, A., Holz, A. and Renkawitz-Pohl, R.** (1999). Essential genes for myoblast fusion in *Drosophila* embryogenesis. *Mech. Dev.* **83**, 17-26.
- Ranganayakulu, G., Zhao, B., Dokidis, A., Molkentin, J. D., Olson, E. N. and Schulz, R. A.** (1995). A series of mutations in the D-MEF2 transcription factor reveal multiple functions in larval and adult myogenesis in *Drosophila*. *Dev. Biol.* **171**, 169-181.
- Robertson, H. M., Preston, C.R., Phillis, R. W., Johnson, S.D., Benz, W.K., Engels, W.R.** (1988). A stable genomic source of P-element transposase in *Drosophila melanogaster*. *Genetics* **118**, 461-470.
- Rothwell, W. F. and Sullivan, W.** (2000). Fluorescent analysis of *Drosophila* embryos. In *Drosophila Protocols* (ed. W. Sullivan, M. Ashburner and R. S. Hawley), pp. 141-158. Cold Spring Harbor, NY: Cold Spring Harbor Laboratory Press.
- Rubin, G. M., Hong, L., Brokstein, P., Evans-Holm, M., Frise, E., Stapleton, M. and Harvey, D. A.** (2000). A *Drosophila* complementary DNA resource. *Science* **287**, 2222-2224.
- Ruiz-Gomez, M. and Bate, M.** (1997). Segregation of myogenic lineages in *Drosophila* requires Numb. *Development* **124**, 4857-4866.
- Ruiz-Gómez, M., Romani, S., Hartmann, C., Jäckle, H. and Bate, M.** (1997). Specific muscle identities are regulated by *Krüppel* during *Drosophila* embryogenesis. *Development* **124**, 3407-3414.
- Ruiz-Gómez, M., Coutts, N., Price A., Taylor, M.V. and Bate, M.** (2000). *Drosophila* Dumbfounded: a myoblast attractant essential for fusion. *Cell* **102**, 189-198.
- Rushton, E., Drysdale, R., Abmayr, S. M., Michelson, A. M. and Bate, M.** (1995). Mutations in a novel gene, *myoblast city*, provide evidence in support of the founder cell hypothesis for *Drosophila* muscle development. *Development* **121**, 1979-1988.
- San Martin, B., Ruiz-Gomez, M., Landgraf, M. and Bate, M.** (2001). A distinct set of founders and fusion-competent myoblasts make visceral muscles in the *Drosophila* embryo. *Development* **128**, 3331-3338.
- Shih, N., Li, J., Karpitskii, V., Nguyen, A., Dustin, M., Kanagawa, O., Miner, J. and Shaw, A.** (1999). Congenital nephrotic syndrome in mice lacking CD2-associated protein. *Science* **286**, 312-315.
- Spradling, A. and Rubin, G.** (1982). Transposition of cloned P elements into *Drosophila* germ line chromosomes. *Science* **218**, 341-347.
- Strunkelnberg, M., Bonengel, B., Moda, L., Hertenstein, A., Ramos, R. G. P., de Couet, H. G. and Fischback, K. F.** (2001). The *irregular chiasm C-roughest* locus and its paralogue, *kin-of-irreC* (*kirre*) are both required and act redundantly during embryonic muscle development of *Drosophila*. In *42nd Annual Drosophila Research Conference*. Washington DC.
- Taillebourg, E. and Dura, J. M.** (1999). A novel mechanism for P element homing in *Drosophila*. *Proc. Natl. Acad. Sci. USA* **96**, 6856-6861.
- Taylor, M. V.** (2000). Muscle development: molecules of myoblast fusion. *Curr. Biol.* **10**, R646-R648.
- Wilson, R.** (1999). Competent steps in determination of cell fate. *BioEssays* **21**, 455-458.